

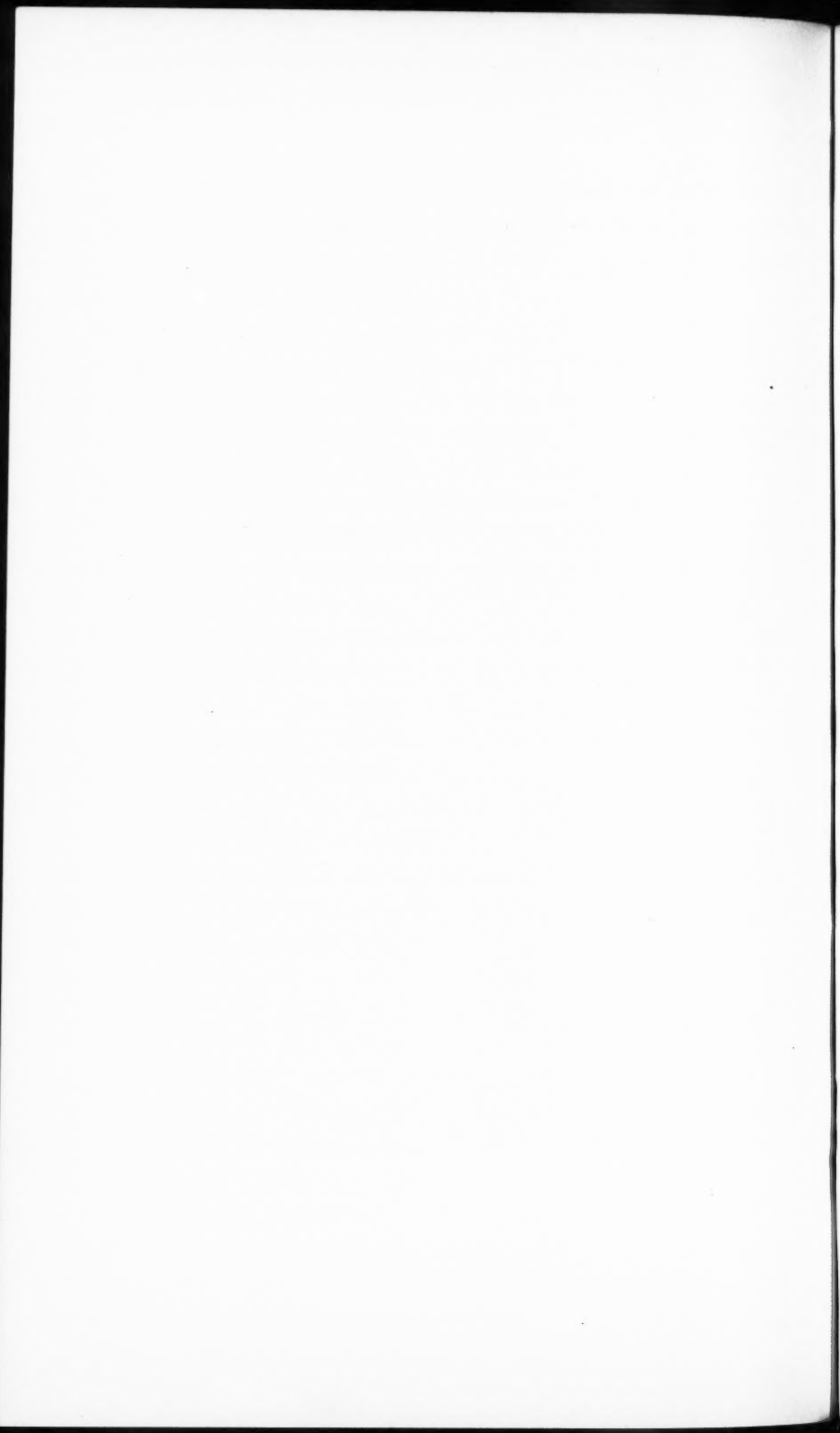
**Proceedings of the American Academy of Arts and Sciences.**

**VOL. 60. No. 10.—OCTOBER, 1925.**

---

**COMPUTATION OF BEHAVIOR OF ELECTRIC  
FILTERS UNDER LOAD.**

**BY A. E. KENNELLY AND ARTHUR SLEPIAN.**



## COMPUTATION OF THE BEHAVIOR OF ELECTRIC FILTERS UNDER LOAD.

By A. E. KENNELLY AND ARTHUR SLEPIAN.

Presented January 14, 1925.

Received January 15, 1925.

### OBJECT OF THE PAPER.

In the quantitative discussion of the behavior of an alternating-current electric filter under variable impressed frequency, it has commonly been assumed<sup>1</sup> that the load at the receiving end has an impedance equal to the characteristic or surge impedance of the filter; in other words that it behaves as though the load at the receiving end was an indefinite prolongation of the same filter. It is proposed to consider a case of a simple uniform, low-pass, five-section filter, with a constant load at the receiving end, and to indicate that in the case of such a relatively high degree of complexity, the behavior of the filter can be readily computed on the principle of simple alternating-current artificial lines.

The results have been obtained by calculation only, as the assumed filter was not actually tested or constructed. A sufficient number of observations have, however, been collected upon actual filters of the same type, to justify reporting the computations. As is customary in such calculations, the filter has been assumed as operating without internal losses or dissipation of power. If, however, definite small uniform resistance and dielectric losses had been assumed, corresponding to those which occur in filters actually employed, the computations would not thereby have been made much more difficult. While they would have taken a little more time to work out, the difference in such a case as this would not be great. The method here indicated is recommended as of general and convenient application.

### PARTICULARS CONCERNING THE FILTER SELECTED FOR COMPUTATION.

Fig. 1 represents the *T* section selected. It has an inductance of  $\mathcal{L} = 0.040$  henry in the series element *AOB*, and a capacitance of  $C = 10^{-6}$  farad, or 1 microfarad, in shunt. The resistance of the inductor is taken as negligible, and likewise the leakance of the condenser.

Fig. 2 represents the series connection of 5 such identical *T* filter sections. The filter is thus assumed to contain a total series induct-

---

<sup>1</sup> One case has however already been briefly reported by F. S. Dellenbaugh, using the method described in this paper. See Bibliography 10, p. 21, Fig. 11.

ance of 0.2 henry, and a total shunt capacitance of 5 microfarads. The load  $\sigma$  between the receiving-end terminal  $B$  and the ground is a constant resistance of 183.3 ohms, either alone, or in series with a constant inductance of 0.0265 henry, according to the position of the switch  $S$ .

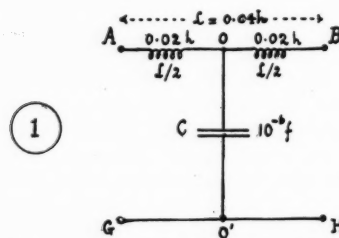


FIG. 1. Section of the Low-Pass Filter Selected.

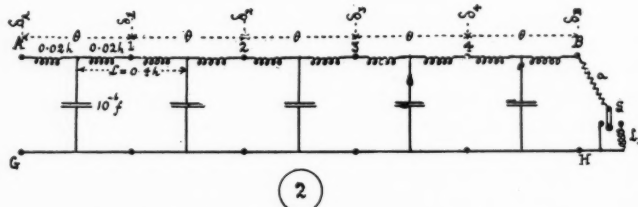


FIG. 2. Five-Section Low-Pass Filter corresponding to the Constants of Fig. 1 with a Load  $\sigma$  at the Receiving end  $B$ .

It is well known that, at a given impressed frequency, the behavior of any symmetrical filter depends on two and only two quantities connected therewith; namely, (1) the hyperbolic angle  $\theta$  of the filter and (2) its surge impedance  $z_0$ , ohms  $\angle$ . Both  $\theta$  and  $z_0$  vary with the frequency. Moreover, in the case of a filter like that of Fig. 2, containing  $n$  identical symmetrical sections, each section will have the same angle  $\theta$ , and surge impedance  $z_0$  so that

$$\Theta = n\theta \quad \begin{matrix} \text{hyperbolic} \\ \text{radians or hyps} \end{matrix} \angle \quad (1)$$

According to the rule<sup>2</sup> for determining the angular velocity of cut off in a filter like that of Figs. 1 and 2, if  $L$  is the series inductance

<sup>2</sup> Bibliography, 2, 6.

in henrys per section, and  $C$  is the shunt capacitance in farads per section,

$$\omega_0 = \frac{2}{\sqrt{LC}} = 2\pi f_0 \quad \frac{\text{radians}}{\text{sec.}} \quad (2)$$

$f_0$  being the cut-off frequency.

If the angular velocity impressed on the filter is  $\omega$ , we may call the ratio of this to the cut-off angular velocity, the frequency ratio  $u$ , or

$$u = \frac{\omega}{\omega_0} = \frac{\omega\sqrt{LC}}{2} = \pi f\sqrt{LC} = \frac{f}{f_0} \quad \text{numeric} \quad (3)$$

This type of filter allows alternating currents to pass for values of the frequency ratio is less than unity, and arrests them more or less completely when this ratio exceeds unity.

At any impressed frequency ratio  $\omega$ , the section angle of this type of filter is defined by the relation

$$\sinh \frac{\theta}{2} = ju \quad \text{numeric} \angle \quad (4)$$

or

$$\theta = 2 \sinh^{-1}(ju) \quad \text{hyp.} \angle \quad (5)$$

Fig. 3 shows a portion of a chart<sup>3</sup> for obtaining antihyperbolic sines, or  $\sinh^{-1}x$ . At  $A$  is the origin of coördinates. Entering the chart on the rectangular coördinate network, we start from  $A$  and move up along the  $j$  line  $ABC$ , until we reach the value chosen for  $u$ . Holding this point with a blunt needle, we read off its corresponding value on the curvilinear coördinates, which are of the type  $x + jq$ . The real component  $x$  is in hyperbolic radians. The  $j$  component  $q$  is in circular quadrants of arc, each quadrant being  $90^\circ$ .

On page 465 is a brief Table of  $\sinh^{-1}(ju)$ , as obtainable from the chart Fig. 3, but to a lower degree of precision.

It will be seen that as  $u$  increases from 0 to 1.0,  $\theta$  increases from  $0 + j0$  to  $0 + j2$  in quadrant measure, or to  $0 + j\pi$  in circular measure. This means that  $\theta$  is entirely imaginary, or has no real component, as far as  $u = 1.0$ . Immediately on passing  $u = 1$ , however, the value of  $\theta$  undergoes no further change in the imaginary part  $j\theta_2$ ; but rapidly develops a real part  $\theta_1$ . An artificial line section of angle  $\theta$ , forming part of an indefinitely long line, subjects any voltage or current which traverses it to an attenuation  $\varepsilon^{-\theta} = \varepsilon^{-(\theta_1 + j\theta_2)} = \varepsilon^{-\theta_1} \searrow \theta_2$ , where  $\varepsilon = 2.718 \dots$  the Napierian base.

---

<sup>3</sup> Bibliography 4.

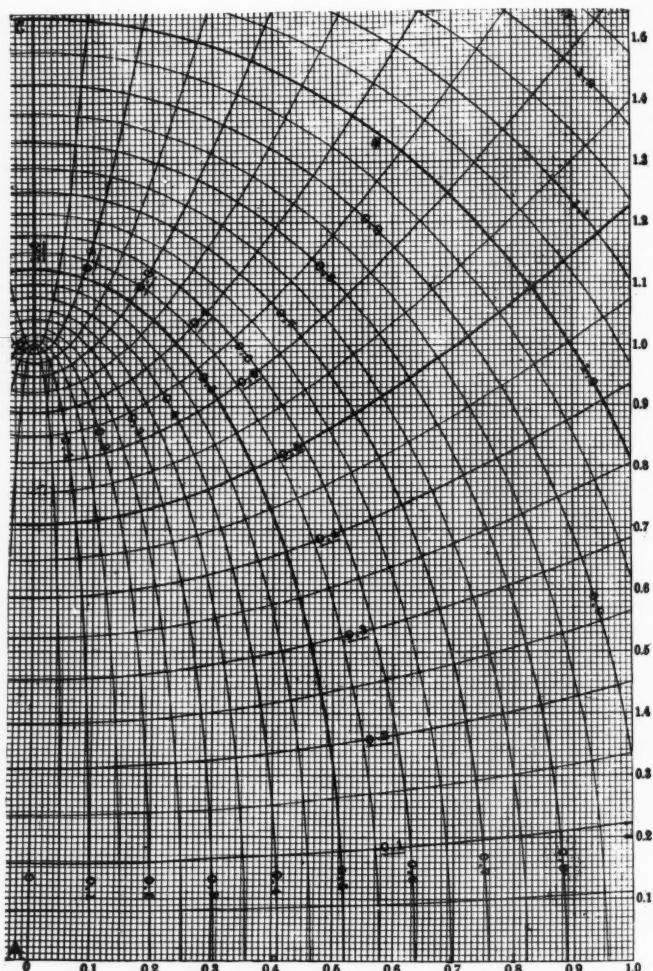


FIG. 3. Portion of Chart for evaluating  $\sinh^{-1} jy = \frac{\theta_1 + j\theta_2}{2}$ .

TABLE I  
SECTION ANGLE  $\theta$  FOR A T-FILTER OF THE TYPE SHOWN IN FIG. 1 AS A FUNCTION OF THE FREQUENCY RATIO  $u$ .

$\omega$	$ju = \frac{\theta_0}{\omega_0}$	$\frac{\theta}{2} = \sinh^{-1}(ju)$		$\theta_1 + j\theta_2$		$\theta = \theta_1 + j\theta_2$	
		quadrants	cir. radians	quadrants	cir. radians	quadrants	cir. radians
0	0	$\frac{\theta_1}{2} + j\frac{\theta_2}{2}$	$\frac{\theta_1}{2} + j\frac{\theta_2}{2}$	$0 + j0$	$0 + j0$	$0 + j0$	$0 + j0$
1000	$j0.1$	$0 + j0$	$0 + j0.0638$	$0 + j0.1002$	$0 + j0.1276$	$0 + j0.2004$	$0 + j0.2004$
2000	$j0.2$	$0 + j0$	$0 + j0.1282$	$0 + j0.2014$	$0 + j0.2566$	$0 + j0.4028$	$0 + j0.4028$
3000	$j0.3$	$0 + j0$	$0 + j0.194$	$0 + j0.3047$	$0 + j0.388$	$0 + j0.6064$	$0 + j0.6064$
4000	$j0.4$	$0 + j0$	$0 + j0.262$	$0 + j0.4115$	$0 + j0.524$	$0 + j0.8230$	$0 + j0.8230$
5000	$j0.5$	$0 + j0$	$0 + j0.333$	$0 + j0.5236$	$0 + j0.666$	$0 + j1.0472$	$0 + j1.0472$
6000	$j0.6$	$0 + j0$	$0 + j0.4095$	$0 + j0.6435$	$0 + j0.819$	$0 + j1.2870$	$0 + j1.2870$
7000	$j0.7$	$0 + j0$	$0 + j0.493$	$0 + j0.7753$	$0 + j0.986$	$0 + j1.5506$	$0 + j1.5506$
8000	$j0.8$	$0 + j0$	$0 + j0.590$	$0 + j0.9273$	$0 + j1.180$	$0 + j1.8546$	$0 + j1.8546$
8100	$j0.81$	$0 + j0$	$0 + j0.601$	$0 + j0.9442$	$0 + j1.202$	$0 + j1.8884$	$0 + j1.8884$
9000	$j0.9$	$0 + j0$	$0 + j0.712$	$0 + j1.1197$	$0 + j1.424$	$0 + j2.2394$	$0 + j2.2394$
10000	$j1.0$	$0 + j0$	$0 + j1.0$	$0 + j1.5708$	$0 + j2.0$	$0 + j3.1416$	$0 + j3.1416$
11000	$j1.1$	$0 + j0$	$0 + j1.0$	$0.4436 + j1.5708$	$0.8872 + j2.0$	$0.8872 + j3.1416$	$0.8872 + j3.1416$
12000	$j1.2$	$0 + j0$	$0.6223 + j1.0$	$0.6223 + j1.5708$	$1.2446 + j2.0$	$1.2446 + j3.1416$	$1.2446 + j3.1416$
13000	$j1.3$	$0 + j0$	$0.7565 + j1.0$	$0.7565 + j1.5708$	$1.513 + j2.0$	$1.513 + j3.1416$	$1.513 + j3.1416$
14000	$j1.4$	$0 + j0$	$0.8670 + j1.0$	$0.8670 + j1.5708$	$1.734 + j2.0$	$1.734 + j3.1416$	$1.734 + j3.1416$
15000	$j1.5$	$0 + j0$	$0.9624 + j1.0$	$0.9624 + j1.5708$	$1.9248 + j2.0$	$1.9248 + j3.1416$	$1.9248 + j3.1416$

Consequently if  $\theta_1$  vanishes,  $\varepsilon^{-\theta} = \varepsilon^{-j\theta_2} = 1 \angle \theta_2$  a mere versor, or phase-shifting operator, causing the voltage or current at its receiving-end terminals to lag in phase  $\theta_2$  circular radians with respect to the corresponding quantity at sending-end terminals; without altering the magnitude or size of the traversing quantity. When, however, there is a real component  $\theta_1$ , not only is there slope attenuation (in phase) but there is also size attenuation (in magnitude). At  $u = 1.5$ , for example,  $\theta = 1.9248 + j\frac{1}{2}$  and  $\varepsilon^{-\theta} = \varepsilon^{-1.9248-j\frac{1}{2}} = 0.146 \angle 180^\circ$ . The voltage or the current will fall in this case to 14.6 per cent in size, and by  $180^\circ$  in slope, when passing through the filter section, provided that there are a large number of similar sections beyond.

In the case of the particular values of  $L$  and  $C$  shown in the  $T$  section of Fig. 1, the cut-off frequency  $\omega_0 = 10,000$  radians per second, ( $f_0 = 1591 \text{ cps}$ ) by (2). The values of impressed angular velocity are then given in the last column of Table I.

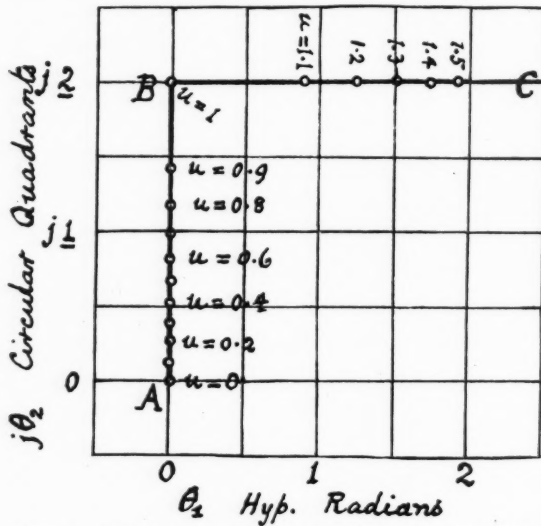


FIG. 4. Vector Locus of Section Angle  $\theta$  as the impressed frequency ratio  $u$  is varied from 0 to 1.5.

Fig. 4 is a vector diagram of the section angle  $\theta$  for the filter Fig. 1, as a function of impressed frequency ratio  $u$ . The vector locus is a pair of perpendicular straight lines,  $AB$  and  $BC$ . The turning point

at  $u = 1$  corresponds to the cut off angular velocity  $\omega_0$ . As  $u$  is increased from 1.5 to infinity, the horizontal locus  $BC$  advances continuously toward the right hand.

The rate of increase of section angle  $\theta$  with respect to a change in  $u$ , is expressed by

$$d\theta = j \frac{2du}{\sqrt{1-u^2}} = j \frac{2du}{\cosh\left(\frac{\theta}{2}\right)} = j \frac{2du}{\cos\left(\frac{\theta_2}{2}\right)} \quad \text{hyp s } \angle \quad (6)$$

below the cut-off value  $u = 1$  and

$$d\theta = \frac{2du}{\sqrt{u^2-1}} = \frac{2du}{\cosh\left(\frac{\theta}{2}\right)} = \frac{2du}{\sinh\left(\frac{\theta_1}{2}\right)} \quad \text{hyp s } \angle \quad (7)$$

beyond the cut-off. Thus, at  $u = 0.8$ , or  $\omega = 8000$  in the case considered,  $d\theta = j2(du/0.6) = j(du/0.3)$ . That is for a small change in  $du$  amounting say to 0.01, or 100 in  $\omega$ ,  $d\theta = j0.033$  hyps; i.e. 0.033 circular radians or 0.0212 quadrant. This is in substantial agreement with the entry in Table I for  $u = 0.81$ .

At  $u_0 = 1$ , or the cut-off frequency,  $d\theta/du$  becomes infinite, which would mean that an indefinitely small change in  $u$  would produce an indefinitely large change in  $\theta$  at this point; but this refers only to a perfect filter devoid of all losses. In the presence of any appreciable loss, the rate of change  $d\theta/du$  becomes finite, but may be large. The larger it is, the better the cut-off behavior of the filter.

#### ANGLE OF MULTIPLE-SECTION FILTER.

Fig. 5 gives the vector locus diagram  $ABC$  of the angle  $\Theta$  subtended by the entire filter of Fig. 2. By comparison with Fig. 4, it will be observed that the effect of the five sections is to make the rate of cut-off five times as great as with a single section. This is known to be a characteristic property of multiple-section filters. That is in changing  $u$  from 1.0 to 1.1, the increase in  $\theta$  is 0.89 hyp. in Fig. 4, and 4.45 in Fig. 5.

#### SURGE IMPEDANCE OF ONE SECTION OR OF THE FIVE-SECTION FILTER.

By the regular rule for determining the surge impedance of a  $T$  section as in Fig. 1,

$$z_0 = \sqrt{\frac{L}{C}} \cosh \frac{\theta}{2} = z_{00} \cosh \frac{\theta}{2} \quad \text{ohms } \angle \quad (8)$$

or in the case considered,  $200 \cosh \theta/2$ , where  $\theta$  is the section angle. The surge impedance thus varies with the impressed frequency.

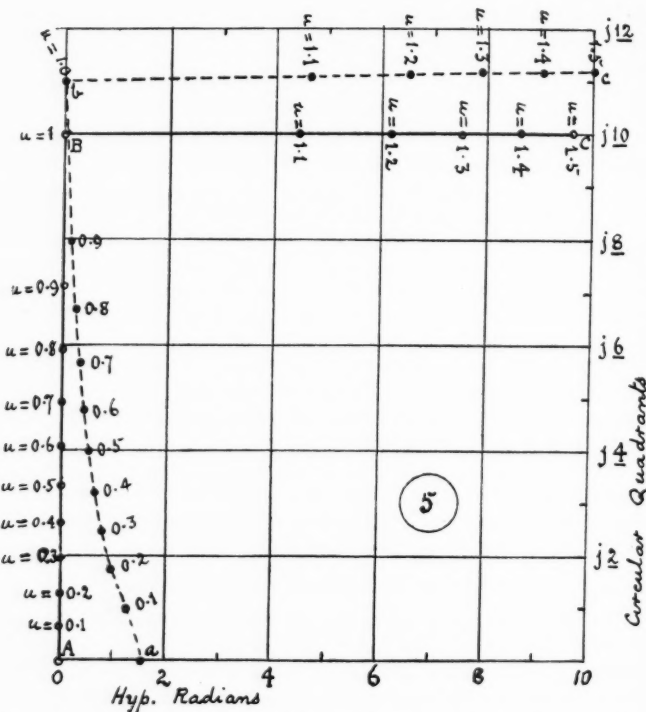


FIG. 5. Vector Locus  $ABC$  of the total filter angle  $\Theta$  as  $u$  varies from 0 to 1.5; also the vector locus  $abc$  of the position angle  $\delta_A$  when the load  $\sigma = 183.3$  ohms + 0.0265 h.

Fig. 6 shows the vector locus. As  $\omega$  increases from 0 to  $\omega_0 = 10,000$ , ( $u = 1$ ),  $z_0$  moves along the graph  $AB$  following the resistance axis from 200 ohms to 0. At the cut-off point,  $z_0$  vanishes, for the case assumed of a lossless filter. From and beyond  $\omega_0$ ,  $z_0$  becomes a pure inductive reactance or  $+j$  quantity, along the branch  $BC$ , increasing rapidly at first, and afterwards more slowly.

POSITION ANGLE  $\delta_B$  AT THE RECEIVING END OF THE  
FILTER UNDER LOAD.

The position angle  $\delta_B$  (Fig. 2) of the receiving end  $B$  of the filter line Fig. 2, under a given load  $\sigma$  ohms  $\angle$  and under an impressed angular velocity  $\omega$ , is equal to the angle  $\theta'$  of that load, and is found from the well known relation

$$\delta_B = \theta' = \theta_1' + j\theta_2' = \tanh^{-1} \frac{\sigma}{z_0} \quad \text{hyp } \angle \quad (9)$$

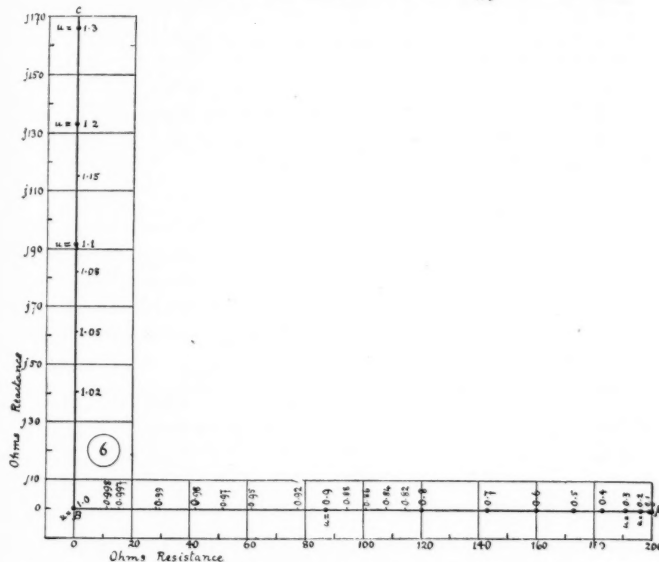


FIG. 6. Vector Locus of the surge impedance  $z_0$  of the filter as the frequency ratio  $u$  is varied from 0 to 1.3 or  $\omega$  from 0 to 13000.

But the impedances  $\sigma$  and  $z_0$  will, in general, vary with the angular velocity  $\omega$ ; so that the angle  $\theta'$  also varies with  $\omega$ . The antitangent of the complex ratio  $\sigma/z_0$  is found from a chart of  $\tanh$  and  $\tanh^{-1}$ . Fig. 7 shows four vector loci of  $\delta_B$  at varying angular velocities, for different loads  $\sigma$  connected to the receiving-end  $B$  of the filter in Fig. 2. The abscissas of Fig. 7 are in real hyperbolic radians  $\theta_1'$ . The ordinates are in circular quadrants of arc ( $j\theta_2'$ ). Thus  $j1.0$  represents one quadrant, ninety degrees, or  $\pi/2$  radians. The four loads  $\sigma$  whose angles  $\theta'$  are plotted in Fig. 7 as a function of  $u$  are:

- (1) A pure resistance load  $\sigma = 183$  ohms, graph  $A b' d' e' D f$ .
- (2) A resistance of 183.3 ohms in series with a condenser of 2.65 microfarads, graph  $D F G H D J K$ .
- (3) A resistance of 183.3 ohms in series with an inductance of 26.5 millihenries, graph  $A B C D E$ .
- (4) A resistance of 156 ohms in series with an inductance of 22.5 millihenries, graph  $a b c D e$ .

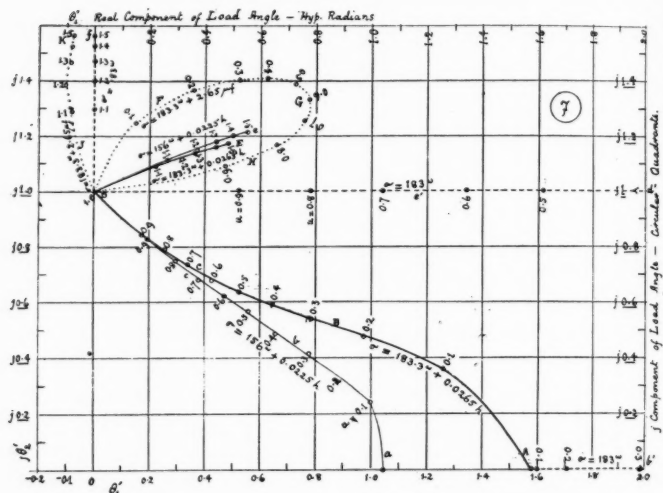


FIG. 7. Vector Loci of  $\delta_B$  or of angles subtended by four different loads  $\sigma$  connected successively to the receiving end  $B$  of the filter shown in Fig. 2.

Different values of  $u$  are marked along each graph. Thus  $u = 0.7$ , corresponding to  $\omega = 7000$  for the filter here discussed, is found near the point  $e'$  on graph 1, near  $G$  on graph 2, and near  $C$  on graphs 3 and 4. Graph 1 for the pure resistance goes off to infinity along the base line as  $\omega$  approaches 4000, or as  $u$  approaches 0.4. It then returns along the parallel line  $d' e' D$  as  $u$  approaches 1.0, then turns sharply through a positive quadrant and follows the straight line  $D f$ .

The load (2) containing the series condenser executes the closed loop  $D F G H D$  and then pursues the curve  $D J K$ .

Loads (3) and (4) pursue somewhat similar curves which change suddenly at  $D$ . This point  $D$  at  $0 + j\frac{1}{2}$  is common to all four graphs at  $u = 1$ , or  $\omega = \omega_0 = 10,000$ . At the cut-off frequency,

therefore, all four loads subtend one circular quadrant when connected to this particular filter in one or more  $T$  sections.

#### POSITION ANGLE $\delta_A$ AT THE SENDING END OF THE FILTER LINE.

In conformity with the regular rule affecting uniform artificial or real lines, operating at a single impressed frequency in the steady state, the position angle at the sending end  $A$ , as shown in Fig. 2, is

$$\delta_A = \Theta + \delta_B = n\theta + \theta' \quad \text{hyp } \angle \quad (10)$$

$\delta_A$  clearly varies with the frequency  $\omega$ , as do both the section angle  $\theta$  and the load angle  $\theta'$ , according to (5) and (9). In Fig. 5, the broken line graph  $a b c$  traces the vector position angle at  $A$  as  $u$  increases from 0 to 1.5.

#### INPUT AND OUTPUT CURRENTS.

If  $I_A$  is the input current at  $A$  (Fig. 2) in rms. amperes, and  $I_B$  the output current given to the load  $\sigma$  at  $B$ , in rms. amperes, we have<sup>4</sup> the well known relation

$$\frac{I_B}{I_A} = \frac{\cosh \delta_B}{\cosh \delta_A} \quad \text{numeric } \angle \quad (11)$$

So that if the input current  $I_A$  is given, the output current  $I_B$  is obtained directly therefrom, with the cosine ratio of the two position angles  $\delta_B$  and  $\delta_A$ . The current strength at any section junction is likewise obtainable from the same rule.

#### INPUT AND OUTPUT IMPEDANCES.

The impedance at and beyond the receiving end  $B$  in Fig. 2, or the output impedance is  $\sigma$  ohms  $\angle$ , a function of the frequency, unless the load  $\sigma$  is a pure resistance. The impedance at the input terminal  $A$ , or the input impedance is well known to be

$$Z_A = z_0 \tanh \delta_A \quad \text{ohms } \angle \quad (12)$$

Both  $z_0$  and  $\delta_A$  vary with the impressed frequency  $f$ . If either the current  $I_A$ , or the emf.  $E_A$  is known at  $A$ , the other can be immediately found from  $Z_A$ .

---

<sup>4</sup> Bibliography, 1, 2, 6.

## INPUT AND OUTPUT VOLTAGES.

The voltages at  $A$  and  $B$  being defined as  $E_A$  and  $E_B$  rms. volts  $\angle$ , the input and output voltages respectively, we have the well known relation

$$\frac{E_B}{E_A} = \frac{\sinh \delta_B}{\sinh \delta_A} \quad \text{numeric } \angle \quad (13)$$

or the output voltage at  $B$  is the input voltage  $E_A$  times the sine ratio of corresponding position angles. The voltage at any intermediate junction can likewise be derived, for any given frequency, by the same rule.

## INPUT AND OUTPUT POWER.

The vector output power  $P_B$  watts  $\angle$  is obtainable directly from the vector output voltage  $E_B$  volts  $\angle$ , and the vector output current  $I_B$  amperes  $\angle$ . This vector power will be expressed either to voltage standard phase, or to current standard phase. In the former case, the voltage  $E_B$  is taken as of zero slope, and the current  $I_B$  is then taken with its slope in local reference thereto. Thus, taking the impressed input voltage  $E_A$  as of initial standard phase say  $10 \angle 0^\circ$  volts, the output voltage  $E_B$  might be say  $8 \angle 600^\circ$  volts, or  $8$  volts  $600^\circ$  in phase behind  $E_A$ ; while the output current  $I_B$  might be say  $0.1 \angle 540^\circ$  amperes, or one-tenth ampere lagging  $540^\circ$  behind  $E_A$ . To find the output power at  $B$ , taking  $E_B$  as of local standard phase, we write

$$E_B = 8 \angle 0^\circ \quad \text{volts } \angle$$

and

$$I_B = 0.1 \angle 60^\circ \quad \text{amperes } \angle$$

because  $I_B$  leads  $E_B$  in phase by  $600 - 540 = 60$  degrees. We then have

$$P_B = E_B \times I_B \quad \text{watts } \angle \quad (14)$$

or in this case  $0.8 \angle 60$  watts  $= 0.4 + j 0.693$  watts; i.e.  $0.4$  watt active, or delivered power, and  $0.693$  watt reactive, or circulating power, of the  $+j$  type, which will represent condensive activity. If, on the other hand, we take the local current at  $B$  as the standard of phase,  $E_B = 8 \angle 60^\circ$  volts, and  $I_B = 0.1 \angle 0^\circ$  ampere, whence by (14),  $P_B = 0.8 \angle 60^\circ$  watt  $= 0.4 - j 0.693$ . The active power is the same as before, but the reactive power is  $-j$ , or condensive.

At the sending-end, with  $E_A$  as phase standard,

$$P_A = E_A \times I_A \quad \text{watts } \angle \quad (15)$$

## BEHAVIOR OF FILTER UNDER SURGE-IMPEDANCE LOAD.

If in Fig. 2, the load  $\sigma$  be kept equal to  $z_0$  as the frequency is changed, the load will behave like an indefinite prolongation of the same filter, or the line becomes infinitely long. The entering current at  $A$ , is then

$$I_A = \frac{E_A}{z_0} = E_A y_0 \quad \text{amperes } \angle \quad (16)$$

or if the impressed voltage is kept at 1 volt, at standard phase, over the entire range of frequency, the entering current will be vectorially equal to the surge admittance  $y_0$ . The voltage and current at  $B$  will then be

$$E_B = E_A \varepsilon^{-\theta} \quad \text{volts } \angle \quad (17)$$

and

$$I_B = I_A \varepsilon^{-\theta} \quad \text{amperes } \angle \quad (18)$$

From an inspection of Figs. (5) and (6), it will be seen that the entering current  $I_A$  will continuously increase as  $\omega$  is varied from 0 to  $\omega_0$ . At the critical frequency  $f_0 = \omega_0/2\pi$ , the entering current will be indefinitely great, or the filter acts like a short circuit, (assuming no internal losses in the filter); while above  $f_0$ , the current falls

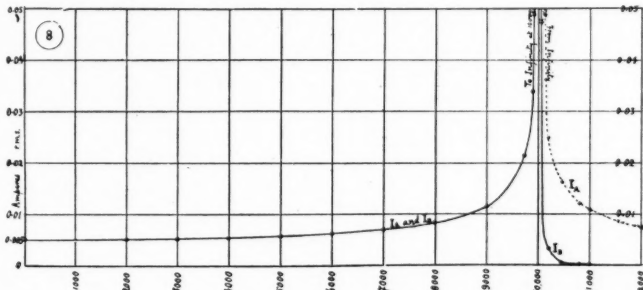


FIG. 8. Current strengths at terminals  $A$  and  $B$  of 5-Section filter Fig. 2 under surge-impedance load  $\sigma = z_0$ , as impressed frequency is varied from  $\omega = 0$  to  $\omega = 12000$ .

off rapidly. This is shown in Fig. 8 by the curve  $I_A$ , commencing at 0.005 ampere with  $\omega = 0$ , and running off the sheet near  $\omega = 9900$ . At  $\omega = 12000$ ,  $I_A$  has returned to 0.075 and is falling. The received current  $I_B$  is numerically equal to  $I_A$  up to the critical frequency. It then falls much faster than  $I_A$  and is very nearly 0 at  $\omega = 11000$

Fig. 9 shows the corresponding vector diagram of  $I_B$  under varying impressed frequency ratio. At zero frequency,  $I_B = PA = 5 \angle 0^\circ$

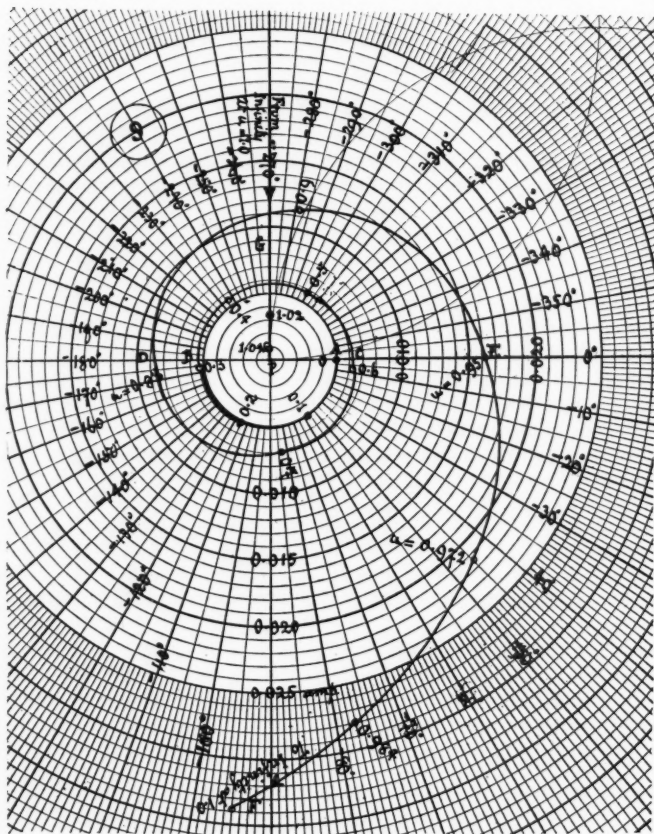


FIG. 9. Vector graph of current  $I_B$  under condition of Surge-Impedance Load.

milliamperes. At  $u = 0.6$  or  $\omega = 6000$ ,  $I_B = OC$  or  $6.25 \angle 368^\circ$  milliamperes. The received current  $I_B$  is then more than one complete cycle behind the impressed emf.  $E_A$ . At  $u = 0.9511$ ,

or  $\omega = 9511$ ,  $I_B = OE = 16 \angle 720^\circ$  milliamperes. At  $OF$ , near  $u = 0.984$ , the received current is  $32 \angle 810^\circ$ , and rapidly increasing. At  $u = 1.0$  it becomes infinite, and above this critical value it returns rapidly along the line  $GP$ . At  $u = 1.02$ , it is  $3.375 \angle 990^\circ$  or 11 quadrants behind  $E_A$  in phase. The entering current  $I_A$  does not pursue this spiral path. As far as  $u = 1$ , it is numerically equal to  $I_B$ , but is in phase with  $E_A$ , or extends along the initial line  $PAE$ .

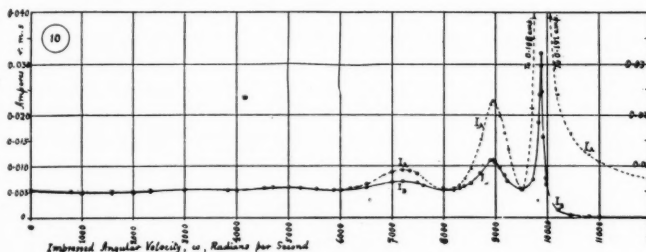


FIG. 10. Current strengths at terminals  $A$  and  $B$  of Five-Section Filter Fig. 2, under Constant-Resistance Load  $\sigma = 183.3$  ohms, as the impressed angular velocity is varied from  $\omega = 0$  to  $\omega = 12000$ .

Above  $u = 1$ ,  $I_A$  returns from infinity along the line  $FP$ , opposite to  $GP$ . Before reaching the critical frequency, therefore, the phase difference between  $I_A$  and  $I_B$  increases from 0 to 10 quadrants or  $900^\circ$ . Beyond  $u = 1$ , it remains constant at 10 quadrants.  $I_B$  falls much more rapidly.

The expanding spiral executed by  $I_B$  in Fig. 9 is, up to  $u = 1$ ,

$$I_B = \frac{y_{00}}{\sqrt{1-u^2}} \angle (2n \sin^{-1} u) = y_{00} \sec \left( \frac{\beta}{2n} \right) \angle \beta \\ = y_{00} \sec \beta' \angle 2n\beta' \quad \text{amperes } \angle \quad (19)$$

where  $y_{00} = \sqrt{C/L}$ , the value of the surge admittance at zero frequency, in this case 0.005,  $n$  is the number of sections in the filter between  $A$  and  $B$ , in this case 5, and  $u = \sin \beta$  and  $\beta' = n\beta$ . This type of expanding spiral may be called the *secant of the 2nth arc* spiral. If we consider a filter made up of a very large number of sections like Fig. 1, the vector current at the junctions 1, 2, 3, . . . in Fig. 2, will be 2nth secant spirals, where  $n = 1, 2, 3, \dots$  successively. Such secant spirals characterize the vector currents at successive junctions along an infinitely long low-pass filter, of the types shown in Figs. 1 and 2.

**BEHAVIOR OF THE FILTER UNDER THE CONSTANT PURE RESISTANCE LOAD  $\sigma = 183.3$  OHMS.**

Fig. 10 shows the corresponding current strengths  $I_A$  and  $I_B$  when the load  $\sigma$  at the receiving end is a constant resistance of 183.3 ohms, as  $\omega$  is increased up to 12000. Instead of having one and only one resonant frequency as in Fig. 8, there are now five resonant frequencies; namely one at  $\omega_0$ , no longer a short-circuit resonance, and lesser resonances at or near  $\omega = 9000, 7000, 5000$  and 3000. There is very little difference between the magnitudes of  $I_A$  and  $I_B$  until the resonance near  $\omega = 7000$  is reached. At this and subsequent resonances,  $I_A$  exceeds  $I_B$ . After reaching the frequency ratio  $u = 0.9877$ , when  $I_A$  goes to 0.191 ampere, and  $I_B$  to 0.032 ampere, both the currents diminish; but  $I_B$  falls much more rapidly. At the cut-off ratio  $u = 1$ ,  $I_B$  has fallen to about 0.006 ampere.

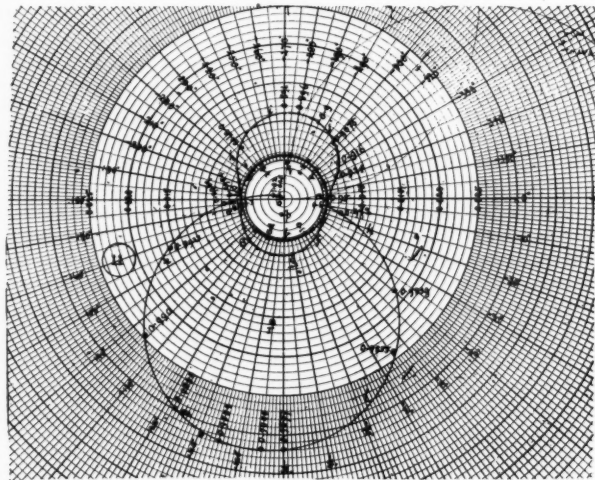


FIG. 11. Vector Graph of Current  $I_B$  under condition of Constant Resistance Load  $\sigma = 183.3$  ohms, as the frequency ratio is increased from  $u = 0$  to  $u = 1.2$ .

The corresponding vector graph of the current  $I_B$  is given in Fig. 11. At  $u = 0$ , this current is 5.4 milliamperes at standard phase, or along the initial line  $oa$ . At  $u = 0.6$ , the current has completed a nearly circular loop  $a b c d$ , and has reached the value  $5.47 \angle 366^\circ.9$ , or

more than 4 quadrants behind the phase of  $E_A$ . It now executes the loop  $f g h j$ , and at  $u = 0.95$ , it has become  $5.46 \angle 720^\circ$  or 8 quadrants in lag. It now executes the nearly circular loop  $k l m n$ , with its diametral maximum near  $u = 0.988$ . At  $u = 1.0$ , it is about 6 milliamperes, 10 quadrants behind  $E_A$  (2 quadrants per section of filter).

The effect of substituting this constant resistance load for the surge-impedance load has been to change the vector graph of  $I_B$  from a secant  $(\beta'/2n)$  spiral, such as that of Fig. 9, to a graph of a succession of approximately circular arcs, as in Fig. 11. The center of the arc  $k l m n$  is at  $r$ , that of  $h i j$  at  $q$ , and that of  $f g$  at  $p$ . These centers lie nearly on one straight line, and fall successively on opposite sides of the origin  $O$ .

Fig. 12. Current strengths at Terminals A and B of Five-section Filter Fig. 2, under Load  $\sigma = 183.3 + j 0.0265 \omega$ .

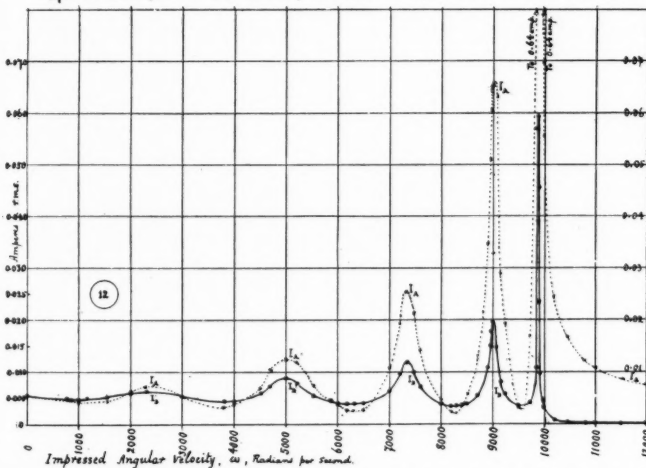


FIG. 12. Current strengths at Terminals A and B of Five-Section Filter Fig. 2, under Load  $\sigma = 183.3 + j 0.0265 \omega$ .

#### BEHAVIOR OF THE FILTER UNDER A CONSTANT REACTIVE LOAD $= 183.3 + j 0.0265$ ohms $\angle$ .

The effect of inserting a pure inductance of 26.5 millihenrys in circuit with 183.3 ohms resistance load, is shown in Fig. 12. The resonances produce in both  $I_A$  and  $I_B$  are now much more marked,

owing to the influence of the inductance in the load. There are five such resonances, one for each section of the filter. The principal resonance is at  $\omega = 9886$ , when  $I_A$  reaches 0.64 ampere, and  $I_B$  0.059 ampere. The other resonances are near  $\omega = 9000, 7350, 5000$  and 2400. At each resonance  $I_A$  exceeds  $I_B$ ; but at intermediate frequencies  $I_A$  falls below  $I_B$ .

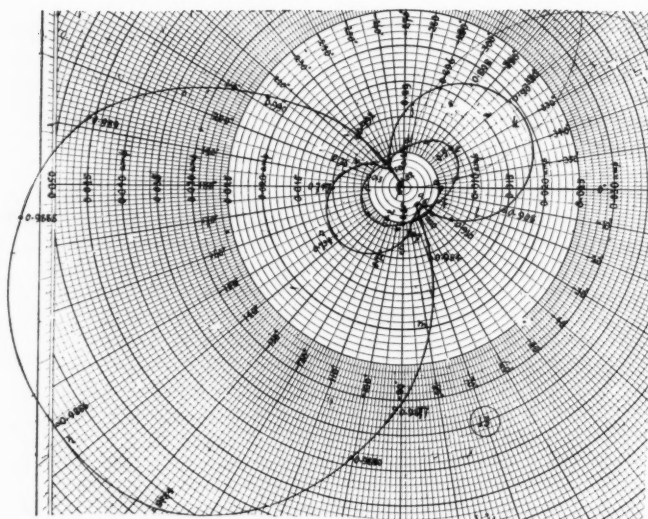


FIG. 13. Vector Graph of Current  $I_B$  under condition of a Reactive Load  $\sigma = 183.3 + j 0.0265 \omega$ , as the frequency ratio is increased from  $u = 0$  to  $u = 1.2$ .

The corresponding vector graph of  $I_B$  appears in Fig. 13.  $ba$  is the initial current at  $u = 0$ . The first half loop  $a b c$ , goes as far as  $u = 0.4$ . The next  $d e f$  reaches  $u = 0.6$ . The third  $g h i$  goes to  $u = 0.8$ . The fourth  $j k l$  reaches  $u = 0.95$ , and the last  $m n o$ , to  $u = 1.02$  and beyond. These loops are only roughly circular, and are not nearly such good approximations to circles as those of Fig. 11. The centers of the loops in Fig. 11 lie nearly on a straight line inclined  $85^\circ$  with the reference axis; but in Fig. 13, the approximate centers lie more nearly on a line  $n p k$ , making an angle of  $30^\circ$  with the reference axis  $p a$ .

It may be noticed that between  $u = 0.984$  and  $u = 0.992$ , the received current is very sensitive to change in impressed frequency, both in regard to magnitude and to phase, or the filter is a sensitive frequency indicator.

Table II indicates, for a few entries only, the method of computation employed, for the case of  $= 183.3 + j0$  ohms, and Table III a few similar examples for the case of  $= 183.3 + j0.0265\omega$ .

#### SUMMARY

(1) Any alternating-current filter, consisting of sections in series having the same surge impedance, forms an artificial electric line, and may advantageously be dealt with, in computation, by means of hyperbolic functions.

(2) The behavior of any such filter under surge-impedance load (virtually infinite line), is apt to be very different from its behavior under a constant load at the receiving end.

(3) In the case of a low-pass inductance-capacitance T-section filter with negligible losses, having a large number of sections, the vector current graphs at  $n$  successive junction points, as the impressed frequency is increased up to cut-off, are expanding secant spirals of the type  $\rho = \rho_0 \sec(\beta/2n)$ .

(4) Under the same conditions last named, but with a constant pure resistance load, the vector received current graph is a close approximation to an aggregation of resonant circles, one for each filter section.

(5) When the load in the last named case includes a constant inductance, the received current graph is a succession of resonant roughly circular loops, one for each filter section.

#### *List of Symbols Employed.*

- $\beta, \beta'$  Circular angles of radius vector in a spiral (radians, quadrants or degrees).
- $C$  Capacitance of a condenser in a filter (farads).
- $\delta_A, \delta_B, \delta_P$  Position angles of terminals  $A$  and  $B$ , or of a junction point  $P$  (hyp  $\angle$ ).
- $E_A, E_B, E_P$  Voltages at terminals  $A$  and  $B$ , or of a junction  $P$  (volts  $\angle$ ).
- $f$  Impressed frequency at the sending end (cyps).
- $f_0$  Cut-off frequency (cyps).
- $\theta = \theta_1 + j\theta_2$  Angle subtended by a filter section (hyp  $\angle$ ).

TABLE II  
EXAMPLES OF TABULAR COMPUTATION OF 5-SECTION FILTER IN FIG. 2, UNDER DIFFERENT SUCCESSIVE FREQUENCIES, WITH  $1.0 \angle 0^\circ$   
VOLT IMPRESSED AT A, AND A LOAD OF 183.3 OHMS AT B.

$u$	$\frac{\theta}{2}$ hyp	$\theta$ hyp	$\Theta_q$ hyp	$\cos \frac{\theta}{2}$	$z_0$ ohms	$\frac{\sigma}{z_0}$	$\bar{z}_B$ hyp	$\bar{z}_A$ hyp	$\tanh \bar{z}_A$	$Z_A =$ $z_0 \tanh \bar{z}_A$ ohms
0.2	$j 0.2014$	$j 0.4028$	$j 1.282$	0.9797	195.9	0.935	1.70	$1.700 + j 1.282$	1.043 $\nabla 3^\circ$ .	204.4 $\nabla 3^\circ.0$
0.4	$j 0.4115$	$j 0.8230$	$j 2.620$	0.9165	183.3	1	$\infty$	$\infty$	1	183.3 $\angle 0^\circ$
0.6	$j 0.6435$	$j 1.287$	$j 4.093$	0.800	160	1.145	$1.347 + j 1$	$1.347 + j 5.093$	1.138 $\nabla 2^\circ.35$	182.2 $\nabla 2^\circ.35$
0.8	$j 0.9273$	$j 1.8546$	$j 5.905$	0.600	120	1.528	$0.783 + j 1$	$0.783 + j 6.905$	$1.490 \angle 7^\circ.5$	178.8 $\angle 7^\circ.5$
0.99	$j 1.429$	$j 2.858$	$j 9.10$	0.141	28.2	6.50	$0.155 + j 1$	$0.155 + j 10.1$	0.220 $\angle 44^\circ$	6.20 $\angle 44^\circ$
$I_A =$ $Z_A = 1/Z_A$ amp $\times 10^{-3}$	$\cosh \bar{z}_A$	$\cosh \bar{z}_B$			$I_B$ amp $\times 10^{-3}$		$\sinh \bar{z}_A$	$\sinh \bar{z}_B$	$E_B$ volts	$\sigma =$ $E_B/I_B$ ohms,
4.892 $\angle 3^\circ.0$	$2.675 \angle 117^\circ$	$2.828 \angle 0^\circ$		$5.172 \nabla 114^\circ$		$2.800 \angle 113^\circ.8$		$2.646 \angle 0^\circ$	$0.945 \nabla 113^\circ.8$	182.7 $\angle 0^\circ.2$
5.455 $\angle 0^\circ$	$\infty$	$\infty$		$5.455 \nabla 235^\circ.8$		$2.055 \angle 97^\circ$		$1$	$235^\circ.8$	183.3 $\angle 0^\circ$
5.488 $\angle 2^\circ.35$	1.80	$\angle 99^\circ.31.793$	$\angle 90^\circ$	$5.467 \nabla 6^\circ.9$				$2.053 \angle 90^\circ.999 \nabla 7^\circ$		182.7 $\nabla 0^\circ.1$
5.593 $\nabla 7^\circ.5$	0.88	$\angle 257^\circ$	$0.8655 \angle 90^\circ$	$5.501 \nabla 174^\circ.5$		$1.315 \nabla 264^\circ.2$		$1.323 \angle 90^\circ.1.006 \nabla 174^\circ.2$		182.8 $\angle 0^\circ.3$
161.2 $\nabla 44^\circ$	1.020 $\angle 182^\circ$	$1.0120 \angle 90^\circ$	24.6 $\nabla 136^\circ$		0.225 $\angle 226^\circ$		0.1556 $\angle 90^\circ.4.498 \nabla 136^\circ$			182.8 $\angle 0^\circ$

TABLE III.  
EXAMPLES OF TABULAR VOLTAGES AND CURRENTS AT SUCCESSIVE TERMINALS OF FIVE-SECTION FILTER IN FIG. 2 WITH LOAD AT  $B$   
OF  $183.3 + j0.0265 \omega$  OHMS, UNDER DIFFERENT IMPRESSED FREQUENCIES.  $E_A = 1.0 \angle 0^\circ$  VOLT.

$u$	$\omega$	$Z_A$	$I_A$	$E_1$	$I_1$	$E_2$	$I_2$
0.2	2000	160.0 $\angle 348^\circ.2$	6.25 $\angle 348^\circ.2$	1.12 $\angle 24^\circ.9$	5.69 $\angle 8^\circ.3$	1.23 $\angle 44^\circ.9$	5.10 $\angle 34^\circ$
0.4	4000	281 $\angle 339^\circ.2$	3.56 $\angle 339^\circ.2$	0.958 $\angle 26^\circ$	3.90 $\angle 54^\circ.5$	0.624 $\angle 76^\circ$	5.53 $\angle 90^\circ.2$
0.6	6000	278 $\angle 34^\circ.3$	3.6 $\angle 34^\circ.3$	0.429 $\angle 91^\circ.3$	6.78 $\angle 83^\circ.7$	1.04 $\angle 166^\circ.8$	3.04 $\angle 143^\circ.7$
0.8	8000	214 $\angle 56^\circ.4$	4.66 $\angle 56^\circ.4$	0.786 $\angle 157^\circ.7$	6.97 $\angle 96^\circ.4$	0.61 $\angle 195^\circ.9$	8.19 $\angle 254^\circ.7$
0.99	9900	3.71 $\angle 67^\circ.8$	268 $\angle 67^\circ.8$	0.88 $\angle 165^\circ.3$	2.20 $\angle 247^\circ.4$	0.73 $\angle 345^\circ.2$	210 $\angle 424^\circ.8$

$E_4$	$I_4$	$E_4$	$I_4$	$E_B$	$I_B$	$\sigma$
volts	millamp.	volts	millamp.	volts	millamp.	ohms
1.26 $\angle 62^\circ.4$	4.86 $\angle 63^\circ.5$	1.22 $\angle 80^\circ.4$	5.46 $\angle 92^\circ.8$	1.10 $\angle 100^\circ.9$	5.85 $\angle 117^\circ$	189.3 $\angle 16^\circ.1$
0.750 $\angle 160^\circ.2$	5.05 $\angle 120^\circ.8$	1.03 $\angle 195^\circ$	3.30 $\angle 173^\circ.2$	0.904 $\angle 214^\circ.2$	4.28 $\angle 244^\circ.3$	211.8 $\angle 30^\circ.1$
0.626 $\angle 208^\circ.3$	6.25 $\angle 249^\circ.2$	0.802 $\angle 330^\circ$	5.17 $\angle 283^\circ.7$	0.946 $\angle 364^\circ.3$	3.89 $\angle 405^\circ.2$	243 $\angle 40^\circ.9$
1.08 $\angle 349^\circ.1$	3.20 $\angle 317^\circ.6$	0.398 $\angle 450^\circ.9$	9.32 $\angle 443^\circ.4$	1.05 $\angle 537^\circ.9$	3.77 $\angle 587^\circ$	280 $\angle 49^\circ.1$
6 $\angle 520^\circ$	157 $\angle 603^\circ.3$	7 $\angle 699^\circ$	93.2 $\angle 783^\circ.3$	7 $\angle 877^\circ.8$	23.1 $\angle 932^\circ.9$	320.5 $\angle 55^\circ.1$

$\theta'$	Angle subtended by a load $\sigma$ at receiving end (hypns $\angle$ ).
$\Theta$	Total angle subtended by a multiple-section filter (hypns $\angle$ ).
$I_A, I_B, I_P$	Current strengths at terminals, or at a junction (amperes $\angle$ ).
$j = \sqrt{-1}$	
$\mathcal{L}$	Inductance in the series branches of a T-filter section (henrys).
$n$	Number of sections in a multiple-section filter.
$\pi = 3.14159\dots$	
$P_A, P_B$	Power at terminals (watts $\angle$ ).
$q$	Imaginary component of a complex angle expressed in circular quadrants.
$\rho$	Radius vector of an expanding spiral.
$\rho_0$	Initial radius vector of an expanding spiral.
$\sigma$	Impedance of a load at receiving end (ohms $\angle$ ).
$u$	Frequency ratio $f/f_0$ (numeric).
$y_0 = 1/z_0$	Surge admittance of a T-filter at a given impressed frequency (ohms $\angle$ ).
$y_{00} = \sqrt{C/\mathcal{L}}$	Surge admittance of T-filter at zero frequency (ohms).
$z_0$	Surge impedance of T-filter at a given impressed frequency (ohms $\angle$ ).
$z_{00} = \sqrt{\mathcal{L}/C}$	Surge impedance of T-filter at zero frequency (ohms).
$\omega = 2\pi f$	Impressed angular velocity (radians per second).
$\omega_0 = 2\pi f_0$	Cut-off angular velocity of filter (radians per second).

## BIBLIOGRAPHY.

(Without pretensions as to completeness).

1. "Artificial Lines for Continuous Currents in the Steady State," A. E. Kennelly. *Proc. Am. Ac. Arts & Sc.*, Nov., 1908, Vol. 44, No. 4, pp. 97-130.
2. "The Application of Hyperbolic Functions to Electrical Engineering Problems," A. E. Kennelly. *University of London Press*, 1911, 3d Ed., 1925, App. R., p. 307.
- 2a. "Wave-Form Sifters for Alternating Currents," A. Campbell. *Proc. Phys. Soc.*, Vol. 24, pp. 107-111, Feb., 1912.
3. "Tables of Complex Hyperbolic and Circular Functions," A. E. Kennelly. *Harvard University Press*, 1913. 2nd Ed. 1921.

4. "Chart Atlas of Complex Hyperbolic and Circular Functions," A. E. Kennelly. *Harvard University Press*, 1913 3rd Ed., 1924.
5. "Note on High-Frequency Wave Filters," G. M. B. Shepherd. *The Electrician*, June 13, 1913, Vol. 71, pp. 399-401
6. "Artificial Electric Lines," A. E. Kennelly. *McGraw-Hill Book Co.*, 1917, Chap. 18.
- 6a. U. S. Patents Nos. 1,227, 113 and 1,227, 114 to G. A. Campbell, May 22, 1914.
- 6b. "Spulen- und Kondensatorleitungen," K. W. Wagner. *Archiv für Elekt.*, Vol. 8, 1919, pp. 61-92.
- 6c. "Reports on Inductive Interference between Electric Power and Communication Circuits" of the Railroad Commission, State of California, April, 1919, pp. 216-217.
7. "Physical Theory of Electric Wave Filter," G. A. Campbell. *The Bell System Technical Journal*, Nov., 1922.
- 6d. "Electric Oscillations and Electric Waves," G. W. Pierce. *Mc Graw-Hill Book Co.*, 1920.
8. "Theory and Design of Uniform and Composite Electric Wave Filters," Otto J. Zobel. *The Bell System Technical Journal*, Jan., 1923, pp. 1-46.
9. "Electric Filter Circuits," Louis Cohen. *Journal of the Franklin Institute*, May, 1923, pp. 641-654.
10. "Electric Filters," F. S. Dellenbaugh, Jr. *Q.S.T.*, July and Aug., 1923.
11. "Theory of Electric Wave Filters Built up of Coupled Circuit Elements," L. J. Peters. *Trans. A.I.E.E.*, February, 1923.
12. "Transient Oscillations in Electric Wave Filters," J. A. Carson and O. J. Zobel. *The Bell System Technical Journal*, July, 1923, pp. 1-52.
13. "Electric Filters," A. Slepian. Thesis Harvard University, June, 1923.



